Kinetic study of dry anaerobic co-digestion of food waste and cardboard for methane production

Gabriel Capson-Tojo, Maxime Rouez, Marion Crest, Eric Trably, Jean-Philippe Steyer, Nicolas Bernet, Jean-Philippe Delgenès, Renaud Escudié

Kinetic study of dry anaerobic co-digestion of food waste and cardboard for methane production

Gabriel Capson-Tojo[1,2], Maxime Rouez[2], Marion Crest[2], Eric Trably[1], Jean-Philippe Steyer[1], Nicolas Bernet[1], Jean-Philippe Delgenès[1], Renaud Escudié[1]*

[a] LBE, INRA, Univ. Montpellier, 102 avenue des Etangs, 11100, Narbonne, France

[b] Suez, CIRSEE, 38 rue du Président Wilson, 78230, Le Pecq, France

* Corresponding author: tel. +33 (0) 468.425.173, e-mail: *renaud.escudie@inra.fr*

Abstract

Dry anaerobic digestion is a promising option for food waste treatment and valorization. However, accumulation of ammonia and volatile fatty acids often occurs, leading to inefficient processes and digestion failure. Co-digestion with cardboard may be a solution to overcome this problem. The effect of the initial substrate to inoculum ratio (0.25 to 1 $gVS \cdot gVS^{-1}$) and the initial total solids contents (20 to 30 %) on the kinetics and performance of dry food waste mono-digestion and co-digestion with cardboard was investigated in batch tests. All the conditions produced methane efficiently (71-93 % of the biochemical methane potential). However, due to lack of methanogenic activity, volatile fatty acids accumulated at the beginning of the digestion and lag phases in the methane production were observed. At increasing substrate to inoculum ratios, the initial acid accumulation was more pronounced and lower cumulative methane yields were obtained. Higher amounts of soluble organic matter remained undegraded at higher substrate loads. Although causing slightly longer lag phases, high initial total solids contents did not jeopardize the methane yields. Cardboard addition reduced acid accumulation and the decline in the yields at increasing substrate loads.

However, cardboard addition also caused higher concentrations of propionic acid, which appeared as the most last acid to be degraded. Nevertheless, dry co-digestion of food waste and cardboard in urban areas is demonstrated as an interesting feasible valorization option.

Keywords

Biomethane; solid-state AD; urban solid waste; microbial adaptation

1. Introduction

The treatment and valorization of food waste (FW) is currently a global issue that needs to be addressed urgently. While traditional methods for FW treatment (*i.e.* landfilling and incineration) are associated with several environmental issues and increasing costs, anaerobic digestion (AD) appears as an effective environmental-friendly industrial process that allows at the same time valorization of the waste into biogas and digestate. From an industrial point of view, AD at high total solid (TS) contents and high loadings is particularly interesting due to the higher associated volumetric biogas production rates (Karthikeyan and Visvanathan, 2013). However, when digesting highly biodegradable substrates rich in nitrogen such as FW, accumulation of volatile fatty acids (VFAs) and free ammonia nitrogen (FAN) usually occurs (Banks et al., 2012, 2008; Capson-Tojo et al., 2016; Zhang et al., 2012a), limiting the loading capacity of the system. This excessive acidification of the digesters may eventually cause a drop of the pH, leading to failure of the digestion process with low methane yields and high chemical oxygen demand (COD) concentrations in the digestates (Capson-Tojo et al., 2016). Different alternatives have been developed recently to avoid VFA accumulation when digesting FW (Capson-Tojo et al., 2016), such as supplementation of trace elements (Zhang et al., 2012b), addition of zero-valent iron (Kong et al., 2016) or co-digestion (Mata-Alvarez et al., 2011). Between those, co-digestion (*i.e.* simultaneous digestion of two or more substrates)

appears as an efficient low-cost option that can be used to avoid accumulation of VFAs. Co-digestion may improve the process by diluting inhibitory compounds, by balancing the C/N ratio and the concentrations of nutrients, by adjusting the moisture content or by increasing the buffering capacity (Mata-Alvarez et al., 2011). Several co-substrates, such as landfill leachate (Liao et al., 2014), paper waste (Kim and Oh, 2011), sewage sludge (Dai et al., 2013), piggery wastewater (Zhang et al., 2011), rice husks (Haider et al., 2015) or green waste (Kumar et al., 2010), have been effectively applied for stabilization of FW AD. Among these options, paper/cardboard waste (CB) can be a suitable co-substrate for FW dry AD, since it has a high C/N ratio, a high TS content and because of its low biodegradability. Furthermore, FW and CB are the two main organic solid waste streams in urban areas (*i.e.*, CB representing up to 35 % of the municipal waste), which facilitates their centralized co-digestion (Hogg et al., 2002; Kim and Oh, 2011; Zhang et al., 2012a).

Besides the potential of this alternative, few studies have been carried out to optimize FW and CB dry co-digestion. At high TS contents (30-50 %) Kim and Oh (2011) used paper waste to adjust the C/N ratio of FW, with a co-digestion ratio of 7:1 g TS FW:g TS CB. They achieved stable methane production (with yields up to 250 ml $CH_4 \cdot g\ COD^{-1}$) without significant VFA accumulation at OLRs up to 10 g $TS \cdot l^{-1} \cdot d^{-1}$. Moreover, Asato et al. (2016) co-digested FW and CB under wet conditions (TS in the inoculum lower than 10 %) at different co-digestion proportions and substrate loadings. Their results showed that mixtures with ≥ 75 % of CB avoided failure of methanogenesis (occurring at concentrations of FW ≥ 18.75 g $COD \cdot l^{-1}$), suggesting that CB addition helped the process operation. In a recent paper at TS contents between 20 to 35 %, Capson-Tojo et al. (2017) concluded that the substrate to inoculum ratio (S/X) and the structure of the microbial community in the inoculum were crucial for an efficient AD process. With an S/X of 0.25 g $VS \cdot g\ VS^{-1}$ methane yields ranging from 307 to 409 ml $CH_4 \cdot g\ VS^{-1}$ were obtained, depending on the FW concentration and the co-digestion

ratio. However, to our knowledge there is no study aiming at understanding the influence of the substrate loading and/or the TS content on the dynamics of VFA production/consumption and the methane yields during dry anaerobic batch co-digestion of FW and CB. As both parameters are critical to assess the feasibility of the AD process and to optimize its performance, their study is essential. Moreover, studying the AD kinetics at dry conditions may potentially lead to a deeper understanding of the process.

Accordingly, the objective of this study was to evaluate the influence of the initial organic load (*i.e.* S/X ratio in batch systems) and the initial TS content on the performance of dry FW mono-digestion and FW co-digestion with CB in batch systems. At the same time, the effect of CB addition itself was also assessed. For the first time under dry conditions using batch reactors, particular attention was paid to the dynamics of VFA production/consumption and methane generation. In addition, the influence of the aforementioned parameters on the final methane yields was assessed. Aiming to elucidate the fate of the organic matter not being transformed into methane, the characteristics of the residual soluble organic matter remaining in the digestates were also studied, as well as the structure of the final microbial communities.

2. Materials and methods

2.1. Substrate and inoculum

A model FW was synthetized according to the VALORGAS report (VALORGAS, 2010) as in Capson-Tojo et al. (2017). Compact cardboard (branded ‘‘Cartonnages Michel’’; shredded to 1 mm) with a density of 1.42 $kg \cdot m^{-3}$ was used as co-substrate. The characteristics of these substrates are shown in Table 1.

The inoculum was collected from an industrial plant treating a mixture of different organic streams. As the concentrations of TAN in the sludge were elevated (5.04 g $TAN \cdot l^{-1}$; pH 8.1; 336 mg $FAN \cdot l^{-1}$), it was assumed that the microbial population were already adapted to high

100 TAN/FAN concentrations (like those found during FW AD). The sludge had a TS content of
101 5.81±0.02 %, with 59.13±0.08 % corresponding to volatile solids (VS).
102 *2.2. Dry batch anaerobic co-digestion*
103 When compared to continuous systems, batch reactors facilitate testing different conditions
104 simultaneously much more easily and therefore they are particularly convenient for AD
105 assays at different TS contents and inoculation ratios. To evaluate the influence of the S/X
106 (*i.e.*, substrate loading), the initial TS content and the substrate composition, eight different
107 conditions were defined (Table 2).
108 The first three reactors (FW-20-0.25, FW-20-0.50, FW-20-100) consisted in mono-digestion batch
109 reactors fed with FW at a given TS content (20 %) and different S/X (0.25, 0.50, 1.0 g VS·g
110 VS^{-1}, respectively). To evaluate the effect of co-digestion, the same conditions were applied
111 in reactors (FW+CB)-20-0.25 to (FW+CB)-20-1.00, but feeding a mixture of FW and CB. The co-
112 digestion ratio was fixed at 7.48 g FW·g CB^{-1} (raw weights), obtaining a substrate with an
113 initial TS content of 30 %. Finally, two other conditions, FW-20-0.25 and $(FW+CB)^{-30-0.25}$,
114 were applied to test the influence of the initial TS content: an S/X of 0.25 g VS·g VS^{-1} was
115 applied, with an initial TS content of 30 %. To adjust the initial TS content in the reactors,
116 dried stabilized compost was added into all the vessels. To correct the endogenous
117 contribution to the biogas from the inoculum and the compost, four different blanks (one per
118 S/X and TS content to consider the influence of the added compost) were carried out.
119 All reactors had a total volume of 2.5 l and were incubated at 35 °C. In order to have similar
120 operating volumes in the reactors (0.6-0.7 l), different initial amounts of FW were added into
121 the vessels. Afterwards, the respective amounts of CB, inoculum and compost (according to
122 Table 2) were supplemented and the mixture was thoroughly homogenized. The headspace
123 volume was determined by measuring the difference in pressure after addition of a known
124 volume of gas and applying the ideal gas law. The reactors were sealed and flushed with

nitrogen to ensure anaerobic conditions. The reactors used were specifically designed to allow sampling of the dry digesting medium during the AD process without disturbing the gas in the head space (Motte et al., 2015). These reactors were equipped with a "ball" valve on their tops, which allowed introducing a metallic sampler. During regular operation, a rubber septum on the top of the valve (opened) allowed monitoring the biogas production. When a sample was to be taken, the valve was closed and the septum was removed. Afterwards, the metallic sampler was fixed over the valve and the sampling volume was flushed with nitrogen. Then, the ball valve was opened, allowing the sampling device to get into the reactor. Once the sample was taken, the valve was closed and the device removed, and, after flushing the empty space with nitrogen, the septum was again placed over the valve. Finally, the valve was opened again. All the conditions were run in duplicate.

2.3. Analytical methods

2.3.1. Physicochemical characterization of the substrates

The TS and VS contents were measured according to the standard methods of the American Public Health Association (APHA, 2005). The protein and carbohydrate concentrations were measured by the modified Lowry method (Frølund et al., 1996) and the Dubois method (Dubois et al., 1956), respectively. A gravimetric method (APHA, 2005) based on accelerated solvent extraction using an ASE®200, DIONEX coupled to a MULTIVAPOR P-12, BUCHI with heptane as solvent (100 bar, 105 °C, 5 cycles of 10 min static and 100s purge) was used to determine the concentrations of lipids. Total Kjeldahl nitrogen (TKN) and NH_4^+ concentrations were measured with an AutoKjehdahl Unit K-370, BUCHI. Total organic carbon (TOC) and inorganic carbon (IC) were determined using a Shimadzu TOC-V_{CSN} Total Organic Carbon Analyzer coupled to a Shimadzu ASI-V tube rack. The total carbon (TC) was calculated as the sum of TOC and IC. The pH was measured by a WTW pHmeter series inoLab pH720. The COD was analyzed using an Aqualytic 420721 COD Vario Tube Test

MR (0-1500 $mg \cdot l^{-1}$). 2 ml of sample were pipetted into each tube and then they were placed inside a HACH COD reactor at 150 °C for 2 h. The COD concentrations were determined using an Aqualytic MultiDirect spectrophotometer. The biochemical methane potentials (BMPs) of the substrates were determined according to Motte et al. (2014).

2.3.2. Gas quantification and analysis

The amount and composition of the biogas produced were determined as described in Cazier et al. (2015). The volumes were normalized (at 0 °C and 1013 hPa) and the endogenous respiration was considered by subtracting the gas generated in the blanks (Cazier et al., 2015).

2.3.3. Analysis of metabolites and final products of the digestion

The concentrations of VFAs, ionic species and other metabolic products (*i.e.*, lactic acid or ethanol) were measured by gas and ion chromatography, according to Cazier et al. (2015) and Motte et al. (2013).

2.4. Microbial community analysis

Samples of the initial inoculum and from the batch reactors at the end of the experiments were analyzed to estimate microbial growth and the structure of the microbial communities. Polymerase Chain Reaction (PCR), quantitative PCR (qPCR) and DNA sequencing techniques were applied. A precise description of the methodology used can be found elsewhere (Moscoviz et al., 2016). According to Moscoviz et al. (2016), the COD equivalent to the microbial growth was calculated assuming average values for the 16S rRNA copies per cell (1.7 for archaea and 4.7 for bacteria) and a chemical composition of the biomass of $C_4H_7O_2N$. Average cell weights were assumed to range between $2.8 \cdot 10^{-13}$ g to $8.0 \cdot 10^{-13}$ g for bacteria (*E. coli*) and between $2.0 \cdot 10^{-13}$ g to $5.8 \cdot 10^{-13}$ g for archaea (*Methanosaeta concilii*) (Milo et al., 2010).

2.5. Fluorescence spectroscopy analysis

The composition and the complexity of the soluble organic matter in the digestates obtained

after AD were assessed by 3 Dimension Excitation Emission Matrix Fluorescence Spectroscopy (3D-EEM). The sample was centrifuged, filtered to 0.45 µm and diluted to a COD concentration of 3-10 $mg \cdot l^{-1}$ (Jimenez et al., 2015). As described in Jimenez et al. (2015), the spectra obtained by 3D-EEM can be decomposed on seven zones according to the fluorescence of each biochemical molecules, which varies according to their complexity. Thus, fluorescent regions I, II and III represent simple compounds and regions IV, V, VI and VII stand for complex matter. The first two regions (Tyrosine-like and Tryptophan-like) represent essential aminoacids and the third region represents soluble microbial products (SMPs), which stand for the pool of organic compounds (*e.g.* polysaccharides, proteins, nucleic acids, organic acids, amino acids, antibiotics, steroids, exocellular enzymes, structural components of cells or products of energy metabolism) that are released during substrate metabolism and biomass decay, excluding VFAs (Barker and Stuckey, 1999). Regions IV, V, VI and VII include complex organic matter usually related with organic matter decay (*i.e.* fulvic and humic acids, regions IV and VII, respectively), large proteins (*i.e.* glycolated proteins, region V) and complex carbohydrate polymers (*i.e.* lignocellulosic matter, region VI). To simplify the results, the distributions of fluorescence from the regions corresponding to simple compounds were added-up. The same was done for the complex organic matter. A technical description of the methodology applied can be found elsewhere (Jimenez et al., 2015).

2.6. Data analysis

The concentration of FAN was calculated as explained in Rajagopal et al. (2013), as a function of temperature, pH, and concentration of TAN. To consider the ionic strength of the media, an activity coefficient was calculated, taking into account the concentrations of the main ions present in the reactors (Cl^-, PO_4^{2-}, Na^+, NH_4^+, K^+, Mg^{2+}, H^+ and Ca^{2+}) (Rajagopal et al., 2013). This approach allowed avoiding an overestimation of the FAN concentrations of up

to 32 % when compared with the ideal solution approach. The yields of methane and metabolites produced during the digestion were progressively corrected according to the amount of digestate sampled for the dynamic analysis. The methane yields were calculated by dividing the volume of methane by the initial mass of VS of substrates (corrected).

Non-linear regression analyses were used to adjust some of the obtained results to theoretical models (*i.e.* modified Gompertz equation) and potential linear correlations between variables were assessed. The least squares method was used in both cases. To evaluate the goodness of fit of non-linear models, the predicted values were plotted against the real data. The resulting R^2 and the p-value obtained from an F-test (determining the percentage of variance explained by the model) were used as indicators.

The cumulative methane productions were fit to the modified Gompertz equation (Zwietering et al., 1990), adjusting the three parameters of the equation: final methane production, (M_{max}, ml CH_4), maximum methane production rate, (R, ml $CH_4 \cdot d^{-1}$), and the lag phase, (L, d). The corresponding expression is shown in Equation 1.

$$M(t) = M_{max} \cdot exp\left\{-exp\left[\frac{R}{M_{max}} \cdot (L - t) + 1\right]\right\} \quad \text{Eq.1}$$

A significance level value of 5 % ($\alpha = 0.05$) was used. The statistical analyses were computed using the statistical software R 3.2.5 (The R Foundation for Statistical Computing, Vienna, Austria). The functions "nls" and "cor" (from the package "corrplot") were used.

3. Results and discussion

3.1. Characterization of substrates

The main characteristics of FW and CB are shown in Table 1.

These characteristics are typical for both substrates. For the model FW, the values are similar to those presented in the literature (Capson-Tojo et al., 2016), with a TS content of 21.6 %

224 and VS/TS of 96.2 %. As it has been also previously reported, this substrate consists mainly
225 of easily degradable carbohydrates, has a high BMP value (498 ml $CH_4 \cdot g\ VS^{-1}$) and a
226 relatively low C/N ratio. On the other hand, CB shows a much higher TS content (92.7 %),
227 consists of hardly degradable carbohydrates (cellulosic compounds) and has a much lower
228 BMP. A more extensive characterization of both substrates can be found in Capson-Tojo et al.
229 (2017).
230 *3.2. Kinetics of the digestion process*
231 Figure 1 presents the dynamic evolution of the cumulated methane productions for the 8
232 operating conditions. Table 3 reports the corresponding kinetic parameters calculated using
233 the Gompertz equation. The high R^2 (≥ 0.994) and the low p-values ($\leq 1.72 \cdot 10^{-21}$) presented
234 in Table 3 suggest a good fit of the experimental results to the Gompertz model applied.
235 At this point, it must be mentioned that all the blanks at 20 % TS were not significantly
236 different (independently of the S/X ratio applied) and had identical kinetics (results not
237 shown), indicating that the added compost did not influence the obtained results. In addition,
238 the gas produced in the blanks represented always less than 10 % of the total gas productions.
239 On the other hand, as the blank at 30 % TS had different kinetics of methane production than
240 the others, this condition was used to estimate the endogenous respiration from reactors FW-
241 30-0.25 and (FW+CB)-30-0.25.
242 The kinetics of methane production clearly depended on the operating conditions. In both
243 mono- and co-digestion reactors, lag phases in the methane production were observed. These
244 lag phases were associated with initial accumulation of VFAs at the beginning of the
245 digestion process (Figure 2). This build-up of acids can be attributed to the high
246 biodegradability of FW. It can be hypothesized that this feature caused a fast FW hydrolysis,
247 with its subsequent conversion into VFAs. In these conditions, the methanogenesis becomes
248 the rate limiting step of the digestion process and VFAs start to accumulate. At greater initial

249 concentrations of FW (higher S/X), more substrate was acidified and the obtained peaks of
250 VFAs were more pronounced, causing greater pH drops (Figure 3). However, the minimum
251 pH value was 7.78, associated with concentrations of VFAs of 22.6 g COD·kg^{-1} (FW-20-
252 1.00). This indicates high buffering capacities in the reactors, higher at greater proportions of
253 CB (lower pH drops). Thus, the pH values were far from being inhibitory for methanogens
254 and cannot explain the lag phases. In fact, even if the lag phases estimated with the Gompertz
255 equation (Table 3) increased with the S/X (from 5.37 to 9.95 with FW as substrate and from
256 4.88 to 10.5 d in the co-digestion reactors), it can be observed that all the curves working at
257 the same TS content are overlapped during the first 10-15 d when looking at the initial phase
258 of methane production (Figure 1). This indicates that the kinetics of methane production were
259 similar during this period. Therefore, it can be stated that the methane production was limited
260 in all the reactors by a lack of methanogenic activity, which led to a rise in the VFA
261 concentrations in the reactors, higher at greater S/X values. After this period, an active
262 community of methanogenic archaea was developed and the VFAs were degraded, producing
263 efficiently methane. In the reactors with TS contents of 30 % (*i.e.* FW-30-0.25 and (FW+CB)-
264 30-0.25), the lower water contents led to slightly higher concentrations of VFAs when
265 compared to reactors at 20 % and the same S/X (*i.e.* FW-20-0.25 and (FW+CB)-20-0.25),
266 causing also slightly lower minimum pH values. In addition, longer lag phases (shown in
267 Figure 1 and Table 3) were observed at 30 % when compared to operation at 20 %. This
268 suggests that the growth of methanogenic archaea was jeopardized at higher TS contents,
269 causing the higher VFA peaks.
270 The initial accumulation of VFAs and the lag phases of methane production observed may
271 have occurred for several reasons. As no irreversible inhibition was observed, the most
272 probable reason might have been the adaptation of the archaea to the initial overloading of
273 substrate. Previous authors have reported long adaptation periods of methanogens (from 0 to

40 d) during AD at high concentrations of TAN/FAN, such those in this study (Van Velsen, 1979). The concentrations of these species in the inoculum were already of 5.04 g $TAN \cdot l^{-1}$ and 336 mg $FAN \cdot l^{-1}$, reaching values up to 5.39±0.24 g $TAN \cdot kg^{-1}$ and 808±44 mg $FAN \cdot kg^{-1}$ in the digestates after AD (Table 5). In addition, these high TAN/FAN concentrations are responsible for the predominance of the hydrogenotrophic pathway for methane production (Banks et al., 2008). Acclimation periods for hydrogenotrophic methanogens similar to those found in this study have also been reported. According to the dilution rate, Ako et al. (2008) reported lag phases of around 5-13 d on the specific methanogenic activities of these microorganisms with inorganic substrates (hydrogen and carbon dioxide) as feed. The values shown in Table 3, ranging from 4.88 to 10.5 d are totally in agreement with those reported in the literature. Therefore, the results suggest that at the beginning of the AD the methanogens were overwhelmed, which led to initial VFA peaks that were greater at higher loadings of substrate. Another fact supporting that the growth of archaea caused the lag phases is that, even if the minimum pH values were higher and the VFA peaks were lower in the reactors co-digesting FW and CB (suggesting less intense VFA accumulation), this was not translated into significantly shorter lag phases, which were similar for both mono- and co-digestion. Another conclusion that can be drawn is the longer adaptation period (longer lag phases) of the methanogens according to the to the TS content.

Despite being clearly within the range reported for inhibition of methanogenesis by TAN/FAN (Chen et al., 2014), efficient methane production was achieved in all the conditions. As most of the TAN was already present in the initial inoculum, no trends were found relating the initial loadings of substrates with the amounts of TAN detected. In fact, irreversible inhibition did not occur besides the high VFA concentrations due to the high TAN/FAN concentrations in the reactors and the high buffering capacity provided by the substrates (mainly CB). If the pH in the reactors had dropped, the VFAs equilibria would have

299 been displaced towards their non-dissociated form (pKa 4.76-4.88), which would have caused
300 severe methanogenic inhibition (Anderson et al., 1982). However, during continuous
301 operation special attention must be paid if high concentrations of acetic acids are maintained
302 at high FAN/TAN concentrations, mainly due to acetogenic inhibition (Banks et al., 2008;
303 Wang et al., 1999).
304 To exemplify more easily the kinetics observed, Figure 4 presents the evolution of the
305 methane yields and the concentrations of individual VFAs in the reactors showing more
306 pronounced initial VFA accumulations (*i.e*. FW-20-1.00 and (FW+CB)-20-1.00; S/X of 1 g
307 $VS \cdot g\ VS^{-1}$).
308 In all the reactors, the main VFA produced was acetic acid, reaching concentrations up to
309 13.6 $g \cdot kg^{-1}$ and 11.7 $g \cdot kg^{-1}$ in reactors FW-20-1.00 and (FW+CB)-20-1.00, respectively.
310 However, this acid, as well as butyric acid, was rapidly consumed when the exponential phase
311 of methanogenesis started. On the other hand, the concentrations of propionic acid continued
312 to increase and it was not consumed until the concentrations of any other VFAs were almost
313 zero. Difficulties for degrading propionate during AD of FW have been previously reported
314 (Banks et al., 2012). During syntrophic acid oxidation and hydrogenotrophic methanogenesis,
315 which is the mechanism supposed to be predominant during high solids AD of FW (Banks et
316 al., 2012; Capson-Tojo et al., 2017), hydrogen and formate act as electron shuttles (Zhao et
317 al., 2016). For propionate oxidation towards acetate to be thermodynamically favorable, the
318 concentrations of hydrogen and formate must be very low (Batstone et al., 2002) and,
319 furthermore, high acetic acid concentrations may also cause a product-induced feedback
320 inhibition of propionate oxidation (Zhao et al., 2016). Therefore, the concentrations of these
321 three compounds must be kept low for propionate to be degraded. This might be the reason of
322 the increasing propionate concentrations reported during continuous AD of FW (Banks et al.,
323 2011). In this study, very low concentrations of hydrogen in the biogas were detected only

during the first 2 days of the AD process (up to 6 % in the gas on the 2nd day and below 0.5 % afterwards), accounting for negligible proportions of the input COD. Controversially, although the addition of CB reduced the intensity of VFAs accumulation, it did not have any beneficial effect on the consumption of propionate. As examples, the concentrations of propionic acid on day 21 in reactors FW-20-1.00 and (FW+CB)-20-1.00 were 2.1 g·kg^{-1} and 2.5 g·kg^{-1}, respectively. The reason for that may be the slower degradability of CB, which may have led to slower production/consumption of the other VFAs, making the oxidation of propionate thermodynamically unfeasible. This may be an issue during long-term co-digestion of FW and CB.

The obtained results suggest that CB can be potentially used in full-scale systems to stabilize FW AD at high TS contents, reducing the TAN/FAN concentrations in the reactors, the VFA peaks and increasing the buffering capacities.

3.3. Overall performance of the digestion

3.3.1. Influence of the operational parameters on the cumulative methane yields

Table 4 shows the experimental methane yields obtained. As it can be observed, while the TS contents did not have any effect on the experimental methane yields (FW-20-0.25 vs. FW-30-0.25 and (FW+CB)-20-0.25 vs. (FW+CB)-30-0.25), the yields decreased when increasing the initial S/X. Lower methane yields at higher substrate loadings have been previously reported using FW as substrate for wet AD. In a co-digestion experiment degrading FW and green waste, Liu et al. (2009) also obtained lower biogas yields at higher S/X. They concluded that, as the final pH values in the reactors were over 7.2, there were no remaining VFAs in the digestate. Therefore, they postulated that either the hydrolysis or the acidogenesis steps were negatively affected at high S/X. However, the fate of the COD not degraded into methane was not discussed and the final concentrations of VFAs in the reactors were not measured. In another study, Kawai et al. (2014) mono-digested FW at different S/X, concluding also that

the methane yield was inversely proportional to this parameter. Moreover, they achieved methane yields over 400 ml $CH_4 \cdot g\ VS^{-1}$ only at S/X lower than 1.0 g $VS \cdot g\ VS^{-1}$. They attributed these lower yields to the so-called "reversible acidification". This term referred to the initial pH drop (lower than 6 in some reactors) caused by initial accumulation of VFAs, which were consumed afterwards. They stated that, when reversible acidification takes place, the final methane yields are often lower than those achieved when this process does not occur. Like in the present study, they did not find any residual VFAs present in the digestate. No explanation was given dealing with the fate of the COD which had not been reduced to methane. Finally, lower methane yields at S/X of 0.25 g $VS \cdot g\ VS^{-1}$ after initial VFA accumulation with FW and CB as substrates were also reported by Capson-Tojo et al. (2017). Concerning the influence of the substrate composition on the methane yields, as the BMP of the CB is lower than that of FW, the methane yields of the co-digestion reactors were lower than those of the mono-digestion systems. In addition, the percentages of the BMP were also lower after CB addition. While for FW the maximum yield corresponded to 93.4±2.9 % of the BMP (S/X of 0.25 g $VS \cdot g\ VS^{-1}$), for co-digestion the maximum was 79.53±7.6 % (also S/X of 0.25 g $VS \cdot g\ VS^{-1}$). This suggests that the supplementation of CB led to a lower conversion of the substrate into methane. However, the addition of CB also diminished the negative impact of higher S/X. While the BMP percentage of FW-20-1.00 was 18 % lower than that of FW-20-0.25, the difference between (FW+CB)-20-1.00 and (FW+CB)-20-0.25 was indeed only 8.5 %.

Other than the lower extent of hydrolysis or acidogenesis, a possible explanation for the lower methane yields at higher substrate loadings may be the same microbial growth and adaptation that caused the lag phases, due to more stressful AD conditions (with higher VFA and TAN concentrations). These processes would uptake COD (otherwise used for methane production) for microbial growth and for the synthesis of extra polymeric substances (EPS) and SMPs (Le

and Stuckey, 2017; Lü et al., 2015). To elucidate this hypothesis, the digestates from the reactors were heavily analyzed.

3.3.2. Analysis carried out to elucidate the fate of the residual organic matter

First of all, in order to test the hypothesis of a more intense microbial growth at higher loadings, qPCRs of the inoculum and the digestates from reactors FW-20-0.25 and FW-20-1.00 were performed. A significant increase in the number of both bacterial and archaeal 16S rRNA operational taxonomic units (OTUs) was found in both reactors when compared to the inoculum. While in the inoculum the number of archaeal and bacterial OTUs were $2.82 \cdot 10^{7}$ $g \cdot g^{-1}$ (wet weight) and $5.87 \cdot 10^{8}$ $g \cdot g^{-1}$, respectively, these numbers were $6.19 \cdot 10^{7}$ $g \cdot g^{-1}$ (archaea) and $3.00 \cdot 10^{9}$ $g \cdot g^{-1}$ (bacteria) and $1.20 \cdot 10^{8}$ $g \cdot g^{-1}$ (archaea) and $4.00 \cdot 10^{9}$ $g \cdot g^{-1}$ (bacteria) in reactors FW-20-0.25 and FW-20-1.00. The number of OTUs was found to be positively correlated to the initial FW concentrations, with R^2 of 0.990 and 0.779 for archaea and bacteria, respectively, indicating a proportional growth of the microorganisms (more intense growth when more substrate was added). It is important to mention that *Methanosarcina* was the main methanogenic species in all the samples, with relative abundances from 53 to 62 % (in accordance with difference studies (Capson-Tojo et al., 2017; Poirier et al., 2016)). These results clearly point out the importance of the initial inoculum for efficient AD batch operation, not only of its composition, but also of the concentrations of microorganisms, which must be in accordance with the FW loading to be applied.

Nevertheless, when considering the amount of COD that this biomass growth could account for, the obtained values for the microbial growth (1.9-5.6 % and 0.8-2.2 % of the total COD supplied as substrate in FW-20-0.25 and FW-20-1.00, respectively) cannot justify the lower methane yields obtained at increasing S/X.

Thus, in an attempt to elucidate the fate of the COD that had neither been transformed into methane nor into biomass, the concentrations of soluble COD (sCOD) remaining in the

399 digestates were measured (Table 5).

400 The sCOD increased linearly with the substrate loadings (R^2 of 0.961 for FW and 0.992 for
401 CB), with values from 7.74±0.52 g COD·kg^{-1} to 10.1±0.89 g COD·kg^{-1} in reactors (FW+CB)-
402 20-0.25 and (FW+CB)-20-1.00, respectively (Table 5). In addition, to take into account the
403 recalcitrant sCOD coming from the inoculum and the compost, the differences between the
404 sCOD in each reactor and the optimum conditions for methane production (*i.e.* FW-20-0.25
405 and (FW+CB)-20-0.25 for each substrate) were calculated. This resulted in increases of the
406 residual sCOD up to 0.627 g·kg^{-1} (FW-20-1.00) for reactors fed with FW and up to 2.37 g·kg^{-1}
407 ((FW+CB)-20-1.00) for the co-digestion reactors. These values (and the concentrations of
408 sCOD presented in Table 5) clearly show that the concentrations of recalcitrant sCOD in the
409 co-digestion systems were much more influenced by the initial loading of substrates than
410 those in the mono-digestion reactors. In fact, when calculating the methane that this sCOD
411 could account for, it represented increments of 5.8 % and 7.4 % of the BMP for (FW+CB)-
412 20-0.50 and (FW+CB)-20-1.00, respectively. Adding this extra methane production
413 (calculated from the measured sCOD) to the experimental methane yields obtained, the
414 differences between the methane yields in the reactors using FW and CB as substrates were
415 negligible at the different S/X tested. This means that the remaining sCOD could explain the
416 difference observed in the methane yields for the co-digestion reactors. However, when
417 repeating these calculations with FW as sole substrate, the increases in the methane yields for
418 FW-20-0.50 and FW-20-1.00 due to the sCOD accounted only for 0.55 % and 1.67 % of the
419 BMP, values far from the differences of 12.1 % and 18 % when compared to FW-20-0.25.
420 Therefore, the amount of sCOD could not explain the decreasing methane yields at higher
421 loadings in the mono-digestion reactors.

422 In an attempt to understand these results, the composition/structure of the sCOD was studied
423 by 3D-EEM, a method that allows estimating the nature of the organic matter. The results

(Table 5) show that although the distributions were similar in all the digestates due to the influence of the initial inoculum (initially much greater mass of sludge and compost was added in comparison to that of substrate), clear tendencies were present. For both substrates, increasing the S/X resulted in higher proportions of simple compounds (related to amino acid/enzyme production and SMPs (Jimenez et al., 2015)) and lower proportions of complex organic matter generally present in stable digestates and composts (coming from the initial inoculum). These differences were more pronounced in the co-digestion reactors, with the fluorescence from simple compounds increasing from 39.3±0.3 % to 48.2±2.0 % and the fluorescence from complex matter decreasing from 60.2±0.3 % to 51.8±2.0 % at increasing S/X ratios. The higher increases in the proportions of simple compounds with CB as co-substrate are in agreement with the results of the sCOD and suggest that this COD might have been used for producing enzymes, amino acids and SMPs required for the digestion process. In comparison, for the mono-digestion experiments, smaller raises in those proportions (as well as in sCOD) were observed at increasing S/X. Putting together the results of the sCOD and the fluorescence analysis, it can be concluded that, even if a more intense production of simple compounds (such as enzymes, amino acids and SMPs) occurred during mono-digestion, it could not explain the lower methane yields in this case. New results have found that, under stressful conditions (particularly at high TAN concentrations), the production of SMPs is much more important than under non-stressed conditions (Le and Stuckey, 2017). In addition to the high TAN/FAN concentrations in all the reactors in this study, higher S/X ratios led to higher transient VFA peaks, which might have led to a more intense synthesis of different simple compounds to favor microbial growth. In addition to these simple compounds, the synthesis of EPS (*i.e.* for biofilm formation) could also explain the decrease in the methane yields at greater loadings (Lü et al., 2015). These COD sinks can remain linked to the solid phase, avoiding their measurement as sCOD. To find out if these

hypotheses are right and the reason of their occurrence, further research must be carried out. In addition, the hypothesis of a less performant hydrolysis step suggested by previous research remains as a feasible possibility (Kawai et al., 2014; Liu et al., 2009). The presented results suggest that the initial structure of the microbial inocula (including the soluble products related to their metabolism) is of critical importance to achieve an efficient AD at high substrate loads, particularly in batch processes and during start-up of full-scale reactors.

4. Conclusions

Efficient methane production was achieved in all the conditions (71-93 % of BMP). However, biomass adaptation led to VFA accumulation and lag phases in the methane production at the beginning of AD. Increasing loadings of substrate caused more pronounced acid accumulations and lower methane yields. Although causing slightly larger lag phases, higher initial TS contents did not jeopardize the methane yields. The addition of cardboard caused less intense acid accumulations and smaller differences in the methane yields at increasing loadings. Propionate was found to be the most recalcitrant acid to be degraded and higher peaks of this acid were observed when CB was added. Higher amounts of simple organic compounds related to microbial metabolism (such as enzymes, amino acids and SMPs) were observed at higher S/X. More research needs to be carried out to elucidate the fate of the organic matter not being transformed into methane neither to sCOD. Nevertheless, if an adapted microbial consortium is used, dry co-digestion of these substrates in urban areas is an interesting feasible valorization option.

Acknowledgement

The authors want to express their gratitude to Suez for financing this research under the CIFRE convention N° 2014/1146. The Communauté d'Agglomération du Grand Narbonne

(CAGN) is also gratefully acknowledged for the financial support. We also wish to thank Diane Ruiz and Clémence Pages for their assistance.

References

Ako, O.Y., Kitamura, Y., Intabon, K., Satake, T., 2008. Steady state characteristics of acclimated hydrogenotrophic methanogens on inorganic substrate in continuous chemostat reactors. Bioresour. Technol. 99, 6305–6310. doi:10.1016/j.biortech.2007.12.016

Anderson, G.K., Donnelly, T., McKeown, K.J., 1982. Identification and control of inhibition in the anaerobic treatment of industrial wastewaters.

APHA, 2005. Standard Methods for the Examination of Water and Wastewater. American Public Health Association, Washington, DC.

Asato, C.M., Gonzalez-Estrella, J., Jerke, A.C., Bang, S.S., Stone, J.J., Gilcrease, P.C., 2016. Batch anaerobic digestion of synthetic military base food waste and cardboard mixtures. Bioresour. Technol. 216, 894–903. doi:10.1016/j.biortech.2016.06.033

Banks, C.J., Chesshire, M., Heaven, S., Arnold, R., 2011. Anaerobic digestion of source-segregated domestic food waste: Performance assessment by mass and energy balance. Bioresour. Technol. 102, 612–620. doi:http://dx.doi.org/10.1016/j.biortech.2010.08.005

Banks, C.J., Chesshire, M., Stringfellow, A., 2008. A pilot-scale trial comparing mesophilic and thermophilic digestion for the stabilisation of source segregated kitchen waste. Water Sci Technol 58, 1475–1481. doi:10.2166/wst.2008.513

Banks, C.J., Zhang, Y., Jiang, Y., Heaven, S., 2012. Trace element requirements for stable food waste digestion at elevated ammonia concentrations. Bioresour. Technol. 104, 127–135. doi:http://dx.doi.org/10.1016/j.biortech.2011.10.068

Barker DJ, Stuckey DC (1999) A Review of Soluble Microbial Products (SMP) in Wastewater Treatment Systems. Water Res. 33, 3063–3082.

Batstone, D.J., Keller, J., Angelidaki, I., Kalyuzhny, S. V, Pavlostathis, S.G., Rozzi, A., Sanders, W.T.M., Siegrist, H., Vavilin, V.A., 2002. Anaerobic digestion model no. 1 (ADM1). IWA Publishing.

Capson-Tojo, G., Rouez, M., Crest, M., Steyer, J.-P., Delgenès, J.-P., Escudié, R., 2016. Food waste valorization via anaerobic processes: a review. Rev. Environ. Sci. Biotechnol. 15, 499–547. doi:10.1007/s11157-016-9405-y

Capson-Tojo, G., Trably, E., Rouez, M., Crest, M., Steyer, J.-P., Delgenès, J.-P., Escudié, R., 2017. Dry anaerobic digestion of food waste and cardboard at different substrate loads, solid contents and co-digestion proportions. Bioresour. Technol. 233, 166-175. doi:10.1016/j.biortech.2017.02.126

Cazier, E.A., Trably, E., Steyer, J.P., Escudie, R., 2015. Biomass hydrolysis inhibition at high hydrogen partial pressure in solid-state anaerobic digestion. Bioresour. Technol. 190, 106–113.

Chen, J.L., Ortiz, R., Steele, T.W.J., Stuckey, D.C., 2014. Toxicants inhibiting anaerobic digestion: a review. Biotechnol. Adv. 32, 1523–34. doi:10.1016/j.biotechadv.2014.10.005

Dai, X., Duan, N., Dong, B., Dai, L., 2013. High-solids anaerobic co-digestion of sewage sludge and food waste in comparison with mono digestions: Stability and performance. Waste Manag. 33, 308–316. doi:http://dx.doi.org/10.1016/j.wasman.2012.10.018

Dubois, M., Gilles, K.A., Hamilton, J.K., Rebers, P.A., Smith, F., 1956. Colorimetric Method for Determination of Sugars and Related Substances. Anal. Chem. 28, 350–356. doi:citeulike-article-id:6244120

Frølund, B., Palmgren, R., Keiding, K., Nielsen, P.H., 1996. Extraction of extracellular polymers from activated sludge using a cation exchange resin. Water research 30, 1749–1758.

Haider, M.R., Zeshan, Yousaf, S., Malik, R.N., Visvanathan, C., 2015. Effect of mixing ratio of food waste and rice husk co-digestion and substrate to inoculum ratio on biogas production.

524 Bioresour. Technol. 190, 451–457. doi:10.1016/j.biortech.2015.02.105
525 Hogg, D., Favoino, E., Nielsen, N., Thompson, J., Wood, K., Penschke, A., Papageorgiou, D.,
526 Economides, S., 2002. Economic analysis of options for managing biodegradable municipal
527 waste, Final Report to the European Commission. Bristol, UNITED KINGDOM.
528 Jimenez, J., Aemig, Q., Doussiet, N., Steyer, J.-P., Houot, S., Patureau, D., 2015. A new
529 organic matter fractionation methodology for organic wastes: bioaccessibility and complexity
530 characterization for treatment optimization. Bioresour. Technol. 194, 344–353.
531 doi:10.1016/j.biortech.2015.07.037
532 Karthikeyan, O.P., Visvanathan, C., 2013. Bio-energy recovery from high-solid organic
533 substrates by dry anaerobic bio-conversion processes: a review. Rev. Environ. Sci.
534 Biotechnol. 12, 257–284.
535 Kawai, M., Nagao, N., Tajima, N., Niwa, C., Matsuyama, T., Toda, T., 2014. The effect of the
536 labile organic fraction in food waste and the substrate/inoculum ratio on anaerobic digestion
537 for a reliable methane yield. Bioresour. Technol. 157, 174–180.
538 doi:http://dx.doi.org/10.1016/j.biortech.2014.01.018
539 Kim, D.-H., Oh, S.-E., 2011. Continuous high-solids anaerobic co-digestion of organic solid
540 wastes under mesophilic conditions. Waste Manag. 31, 1943–1948.
541 doi:http://dx.doi.org/10.1016/j.wasman.2011.05.007
542 Kong, X., Wei, Y., Xu, S., Liu, J., Li, H., Liu, Y., Yu, S., 2016. Inhibiting excessive
543 acidification using zero-valent iron in anaerobic digestion of food waste at high organic load
544 rates. Bioresour. Technol. 211, 65–71. doi:10.1016/j.biortech.2016.03.078
545 Kumar, M., Ou, Y.-L., Lin, J.-G., 2010. Co-composting of green waste and food waste at low
546 C/N ratio. Waste Mang. (New York, N.Y.) 30, 602–9. doi:10.1016/j.wasman.2009.11.023
547 Le, C., Stuckey, D.C., 2017. The Influence of Feeding Composition on The Production of
548 Soluble Microbial Products (SMPs) in Anaerobic Digestion, in: 1st International ABWET

549 Conference : Waste-to-Bioenergy : Applications in Urban Areas. Paris, pp. 116–117.
550 Liao, X., Zhu, S., Zhong, D., Zhu, J., Liao, L., 2014. Anaerobic co-digestion of food waste
551 and landfill leachate in single-phase batch reactors. Waste Manag. 34, 2278–2284.
552 doi:http://dx.doi.org/10.1016/j.wasman.2014.06.014
553 Liu, G., Zhang, R., El-Mashad, H.M., Dong, R., 2009. Effect of feed to inoculum ratios on
554 biogas yields of food and green wastes. Bioresour. Technol. 100, 5103–5108.
555 doi:http://dx.doi.org/10.1016/j.biortech.2009.03.081
556 Lü, F., Zhou, Q., Wu, D., Wang, T., Shao, L., He, P., 2015. Dewaterability of anaerobic
557 digestate from food waste: Relationship with extracellular polymeric substances. Chem. Eng.
558 J. 262, 932–938. doi:http://dx.doi.org/10.1016/j.cej.2014.10.051
559 Mata-Alvarez, J., Dosta, J., Macé, S., Astals, S., 2011. Codigestion of solid wastes: a review
560 of its uses and perspectives including modeling. Crit. Rev. Biotechnol. 31, 99–111.
561 Moscoviz, R., Trably, E., Bernet, N., 2016. Consistent 1,3-propanediol production from
562 glycerol in mixed culture fermentation over a wide range of pH. Biotechnol. Biofuels 9, 32.
563 doi:10.1186/s13068-016-0447-8
564 Milo R., Jorgensen P., Moran U., Weber G., Springer M., 2010. BioNumbers-the database of
565 key numbers in molecular and cell biology. Nucl. Acids Res. 38 (suppl 1): D750-D753.
566 Motte, J.-C., Escudié, R., Beaufils, N., Steyer, J.-P., Bernet, N., Delgenès, J.-P., Dumas, C.,
567 2014. Morphological structures of wheat straw strongly impacts its anaerobic digestion. Ind.
568 Crops and Prod. 52, 695–701.
569 Motte, J.-C., Trably, E., Escudié, R., Hamelin, J., Steyer, J.-P., Bernet, N., Delgenes, J.-P.,
570 Dumas, C., 2013. Total solids content: a key parameter of metabolic pathways in dry
571 anaerobic digestion. Biotechnol. Biofuels 6, 164.
572 Motte, J.-C., Watteau, F., Escudié, R., Steyer, J.-P., Bernet, N., Delgenes, J.-P., Dumas, C.,
573 2015. Dynamic observation of the biodegradation of lignocellulosic tissue under solid-state

574 anaerobic conditions. Bioresour. Technol. 191, 322–326. doi:10.1016/j.biortech.2015.04.130
575 Poirier, S., Desmond-Le Quéméner, E., Madigou, C., Bouchez, T., Chapleur, O., 2016.
576 Anaerobic digestion of biowaste under extreme ammonia concentration: Identification of key
577 microbial phylotypes. Bioresour. Technol. 207, 92–101. doi:10.1016/j.biortech.2016.01.124
578 Rajagopal, R., Massé, D.I., Singh, G., 2013. A critical review on inhibition of anaerobic
579 digestion process by excess ammonia. Bioresource Technology 143, 632–641.
580 doi:http://dx.doi.org/10.1016/j.biortech.2013.06.030VALORGAS, 2010. D2.1: Compositional
581 analysis of food waste from study sites in geographically distinct regions of Europe,
582 Valorisation of food waste to biogas.
583 Van Velsen, A.F.M., 1979. Adaptation of methanogenic sludge to high ammonia-nitrogen
584 concentrations. Water Res. 13, 995–999. doi:10.1016/0043-1354(79)90194-5
585 Wang, Q., Kuninobu, M., Ogawa, H.I., Kato, Y., 1999. Degradation of volatile fatty acids in
586 highly efficient anaerobic digestion. Biomass Bioenergy 16, 407–416. doi:10.1016/S0961-
587 9534(99)00016-1
588 Zhang, L., Lee, Y.-W., Jahng, D., 2011. Anaerobic co-digestion of food waste and piggery
589 wastewater: Focusing on the role of trace elements. Bioresour. Technol. 102, 5048–5059.
590 doi:http://dx.doi.org/10.1016/j.biortech.2011.01.082
591 Zhang, Y., Banks, C.J., Heaven, S., 2012a. Co-digestion of source segregated domestic food
592 waste to improve process stability. Bioresour. Technol. 114, 168–178.
593 doi:http://dx.doi.org/10.1016/j.biortech.2012.03.040
594 Zhang, L., Ouyang, W., Lia, A., 2012b. Essential Role of Trace Elements in Continuous
595 Anaerobic Digestion of Food Waste. Procedia Environ. Sci. 16, 102–111.
596 doi:http://dx.doi.org/10.1016/j.proenv.2012.10.014
597 Zhao, Z., Zhang, Y., Yu, Q., Dang, Y., Li, Y., Quan, X., 2016. Communities stimulated with
598 ethanol to perform direct interspecies electron transfer for syntrophic metabolism of

propionate and butyrate. Water Res. 102, 475–484. doi:10.1016/j.watres.2016.07.005

Zwietering, M.H., Jongenburger, I., Rombouts, F.M., Van't Riet, K., 1990. Modeling of the bacterial growth curve. Appl. Environ. Microbiol. 56, 1875–1881.

Figure and table captions

Figure 1. Evolution of the cumulative methane production during anaerobic mono-digestion of food waste (A) and co-digestion of food waste and cardboard (B). The legend represents the operating conditions: total solid contents (%) and substrate to inoculum ratio (g VS·g VS^{-1})

Figure 2. Concentration of total volatile fatty acids during anaerobic mono-digestion of food waste (A) and co-digestion of food waste and cardboard (B). The legend represents the operating conditions: total solid contents (%) and substrate to inoculum ratio (g VS·g VS^{-1})

Figure 3. Evolution of the pH in the reactors during anaerobic mono-digestion of food waste (A) and co-digestion of food waste and cardboard (B). The legend represents the operating conditions: total solid contents (%) and substrate to inoculum ratio (g VS·g VS^{-1})

Figure 4. Concentrations of volatile fatty acids and methane yields during anaerobic digestion in reactor FW-20-1.00 (A; food waste mono-digestion; substrate to inoculum ratio of 1 g VS·g VS^{-1}; 20 % total solids) and reactor (FW+CB)-20-1.00 (B; food waste and cardboard co-digestion; substrate to inoculum ratio of 1 g VS·g VS^{-1}; 20 % total solids)

Table 1. Main characteristics of the substrates (Capson-Tojo et al., 2017)

Table 2. Experimental design of the batch reactors

Table 3. Best-fitting parameters corresponding to the representation of the cumulative methane productions by the Gompertz equation

Table 4. Experimental results for the final methane yields

Table 5. Concentrations of sCOD, TAN and FAN in the digestates and 3D-EEM results corresponding to the soluble fraction of the digestates

Abbreviations

3D-EEM – 3 Dimension Excitation Emission Matrix Fluorescence Spectroscopy
AD – Anaerobic Digestion
BMP – Biomethane Chemical Potential
CB – Cardboard
COD – Chemical Oxygen Demand
EPS – Extra Polymeric Substances
FAN – Free Ammonia Nitrogen
FW – Food Waste
IC – Inorganic Carbon
L – Lag phase

637 **M_{max}** – Final methane yield
638 **OTU** – Operational Taxonomic Unit
639 **PCR** – Polymerase Chain Reaction
640 **qPCR** – Quantitative Polymerase Chain Reaction
641 **R** – Maximum methane production rate
642 **rRNA** – Ribosomal Ribonucleic Acid
643 **S/X** – Substrate to Inoculum ratio
644 **sCOD** – soluble Chemical Oxygen Demand
645 **SMPs** – soluble metabolic products
646 **TC** – Total Carbon
647 **TKN** – Total Kjeldahl Nitrogen
648 **TOC** – Total Organic Carbon
649 **TS** – Total Solids
650 **VFAs** – Volatile Fatty Acids
651 **VS** – Volatile Solids

Graphical abstract

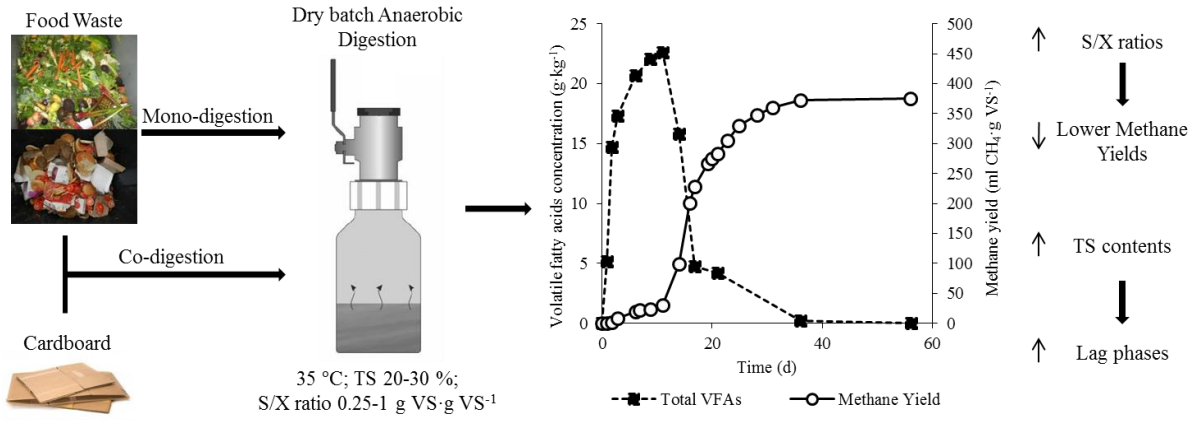

Table1

Table 1. Main characteristics of the substrates (Capson-Tojo et al., 2017)

Parameter/Element	Unit	Food Waste	Cardboard
TS	% (w. b.)	21.6±0.7	92.7±3.7
VS	% TS	96.2±0.1	77.5±0.2
pH	Unit pH	5.60	7.10
COD	g COD·g TS^{-1}	1.37±0.05	1.19±0.05
BMP	ml CH_4·g VS^{-1}	498±42	250±3
NH_4	g·kg TS^{-1}	0.051	0.002
TKN	g·kg TS^{-1}	27.08±1.64	2.00±0.02
TC	g·kg TS^{-1}	442±7	366±6
C/N	$g \cdot g^{-1}$	16.3	183
Carbohydrates	g·kg TS^{-1}	687±15	958±5
Proteins	g·kg TS^{-1}	169±10	0
Lipids	g·kg TS^{-1}	72.3±1.5	0

* TS stands for total solids; VS for volatile solids; COD for chemical oxygen demand; BMP for biochemical methane potential; TKN for total Kjeldahl nitrogen; TC for total carbon

Table 2. Experimental design of the batch reactors

Purpose	# Reactor	TS_0 (%)	S/X (g VS·g VS^{-1})	FW added (g)	CB added (g)	Initial FW concentration (g VS·l^{-1})
FW at 3 S/X	FW-20-0.25	20	0.25	20	0.0	7.07
	FW-20-0.50	20	0.50	40	0.0	13.7
	FW-20-1.00	20	1.00	80	0.0	25.7
FW and CB at 3 S/X	(FW+CB)-20-0.25	20	0.25	15	2.0	4.90
	(FW+CB)-20-0.50	20	0.50	30	4.0	9.57
	(FW+CB)-20-1.00	20	1.00	60	8.0	18.3
Influence TS content	FW-30-0.25	30	0.25	20	0.0	6.19
	(FW+CB)-30-0.25	30	0.25	15	2.0	4.29
Endogenous respiration at different compost proportions	Blank1	20	-	0	0	0
	Blank2	20	-	0	0	0
	Blank3	20	-	0	0	0
	Blank4	30	-	0	0	0

* TS_0 stands for initial total solid content; S/X for substrate to inoculum ratio; VS for volatile solids; FW for food waste; CB for cardboard

Table3

Table 3. Best-fitting parameters corresponding to the representation of the cumulative methane productions by the Gompertz equation

# Reactor	TS_0 (%)	S/X (g VS·g VS^{-1})	Cumulative methane (ml CH_4)	Maximum methane production rate (ml $CH_4 \cdot d^{-1}$)	Lag phase (d)	R^2	p-value F-test
FW-20-0.25	20	0.25	1916	156	5.37	0.997	< 0.0001
FW-20-0.50	20	0.50	3470	279	7.73	0.995	< 0.0001
FW-20-1.00	20	1.00	6241	515	9.95	0.994	< 0.0001
(FW+CB)-20-0.25	20	0.25	1597	124	4.88	0.996	< 0.0001
(FW+CB)-20-0.50	20	0.50	3485	199	6.26	0.994	< 0.0001
(FW+CB)-20-1.00	20	1.00	5800	533	10.5	0.995	< 0.0001
FW-30-0.25	30	0.25	1992	182	8.43	0.998	< 0.0001
(FW+CB)-30-0.25	30	0.25	1563	147	8.22	0.996	< 0.0001

* TS_0 stands for initial total solid content; S/X for substrate to inoculum ratio; FW for food waste; CB for cardboard

Table4

Table 4. Experimental results of the final methane yields

# Reactor	TS_0 (%)	S/X (g VS·g VS^{-1})	Methane yield (ml CH_4·g VS^{-1})	% of BMP
FW-20-0.25	20	0.25	464±14	93.4± 2.9
FW-20-0.50	20	0.50	405±12	81.3± 2.5
FW-20-1.00	20	1.00	375±17	75.4± 6.4
(FW+CB)-20-0.25	20	0.25	334±32	79.5± 7.6
(FW+CB)-20-0.50	20	0.50	321	76.5
(FW+CB)-20-1.00	20	1.00	298	71.0
FW-30-0.25	30	0.25	464±24	93.2± 4.9
(FW+CB)-30-0.25	30	0.25	333±14	79.3± 3.4

* TS_0 stands for initial total solid content; S/X for substrate to inoculum ratio; VS for volatile solids; BMP for biochemical methane potential; FW for food waste; CB for cardboard

Table5

Table 5. Concentrations of sCOD, TAN and FAN in the digestates and 3D-EEM results corresponding to the soluble fraction of the digestates

# Reactor	TS_0 (%)	S/X (g VS·g VS^{-1})	sCOD (g COD·kg^{-1})	TAN (g·kg^{-1})	FAN (mg·kg^{-1})	Fluorescence simple compounds (%)(1)	Fluorescence complex matter (%)(2)
FW-20-0.25	20	0.25	7.75±0.42	4.80±0.47	643±80	41.2±0.1	57.1±3.8
FW-20-0.50	20	0.50	7.84±0.23	5.39±0.24	713±4	41.7±0.4	58.3±0.2
FW-20-1.00	20	1.00	8.38±0.43	5.05±0.16	808±44	44.6±0.8	55.4±1.0
(FW+CB)-20-0.25	20	0.25	7.74±0.52	4.96±0.14	663±2	39.3±0.3	60.2±0.3
(FW+CB)-20-0.50	20	0.50	8.72±1.57	4.93±0.08	803±32	42.1±2.1	57.9±2.1
(FW+CB)-20-1.00	20	1.00	10.1±0.89	4.97±0.15	670± 49	48.2±2.0	51.8±2.0
FW-30-0.25	30	0.25	8.34±0.22	2.62±0.10	419±28	37.3±0.7	62.7±1.3
(FW+CB)-30-0.25	30	0.25	8.26±0.41	3.20±0.22	509±52	40.5±0.5	59.4±0.5

(1) Addition of fluorescence from regions representing simple compounds: I (tyrosine-like simple aromatic proteins), II (tryptophan-like simple aromatic proteins) and III (soluble microbial products)
(2) Addition of fluorescence from regions representing complex matter: IV (fulvic acid-like matter), V (glycolated proteins-like), VI (lignocellulosic-like) and VII (humic acid-like)

Figure1

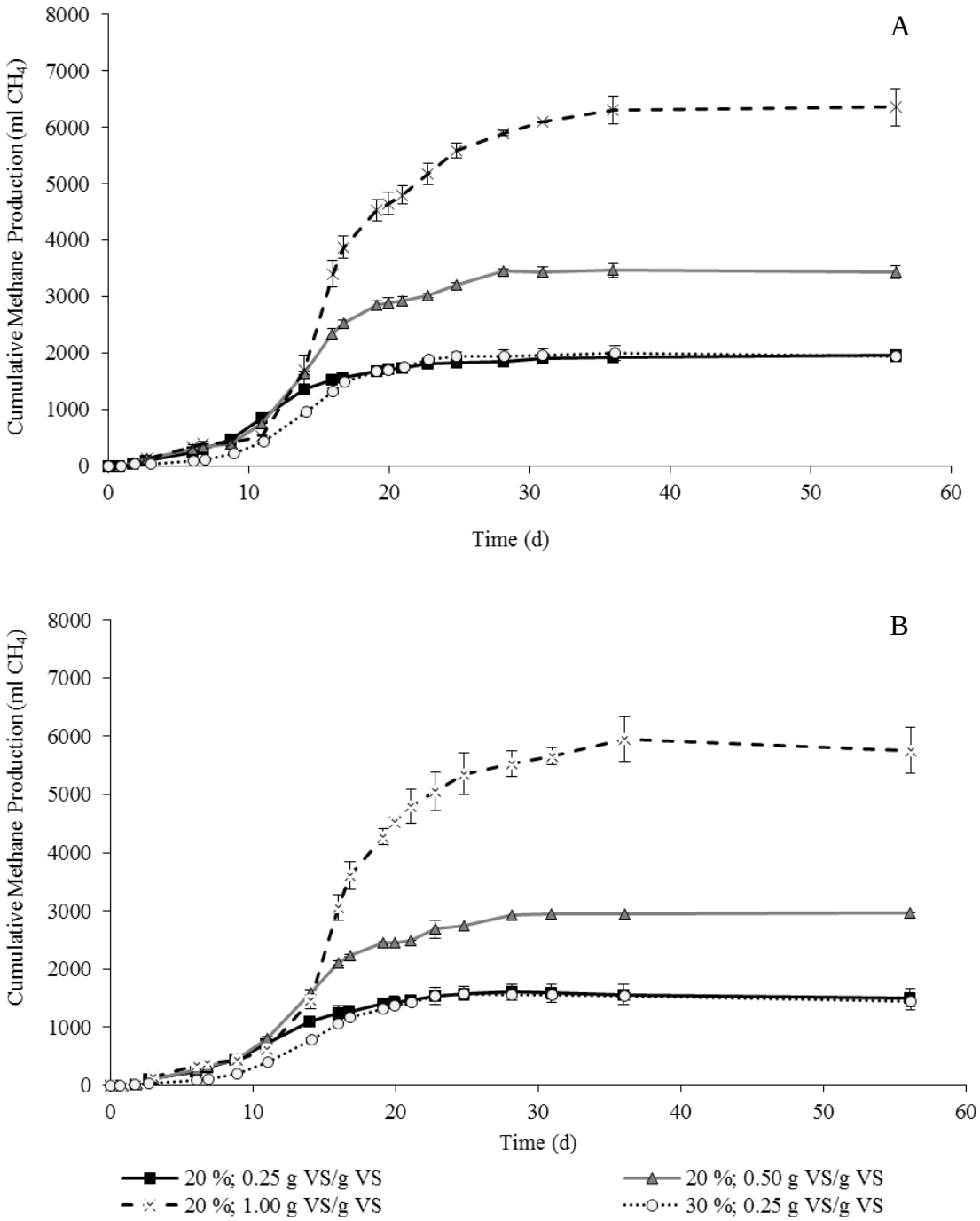

Figure 1. Evolution of the cumulative methane production during anaerobic mono-digestion of food waste (A) and co-digestion of food waste and cardboard (B). The legend represents the operating conditions: total solid contents (%) and substrate to inoculum ratio (g VS·g VS^{-1})

Figure2

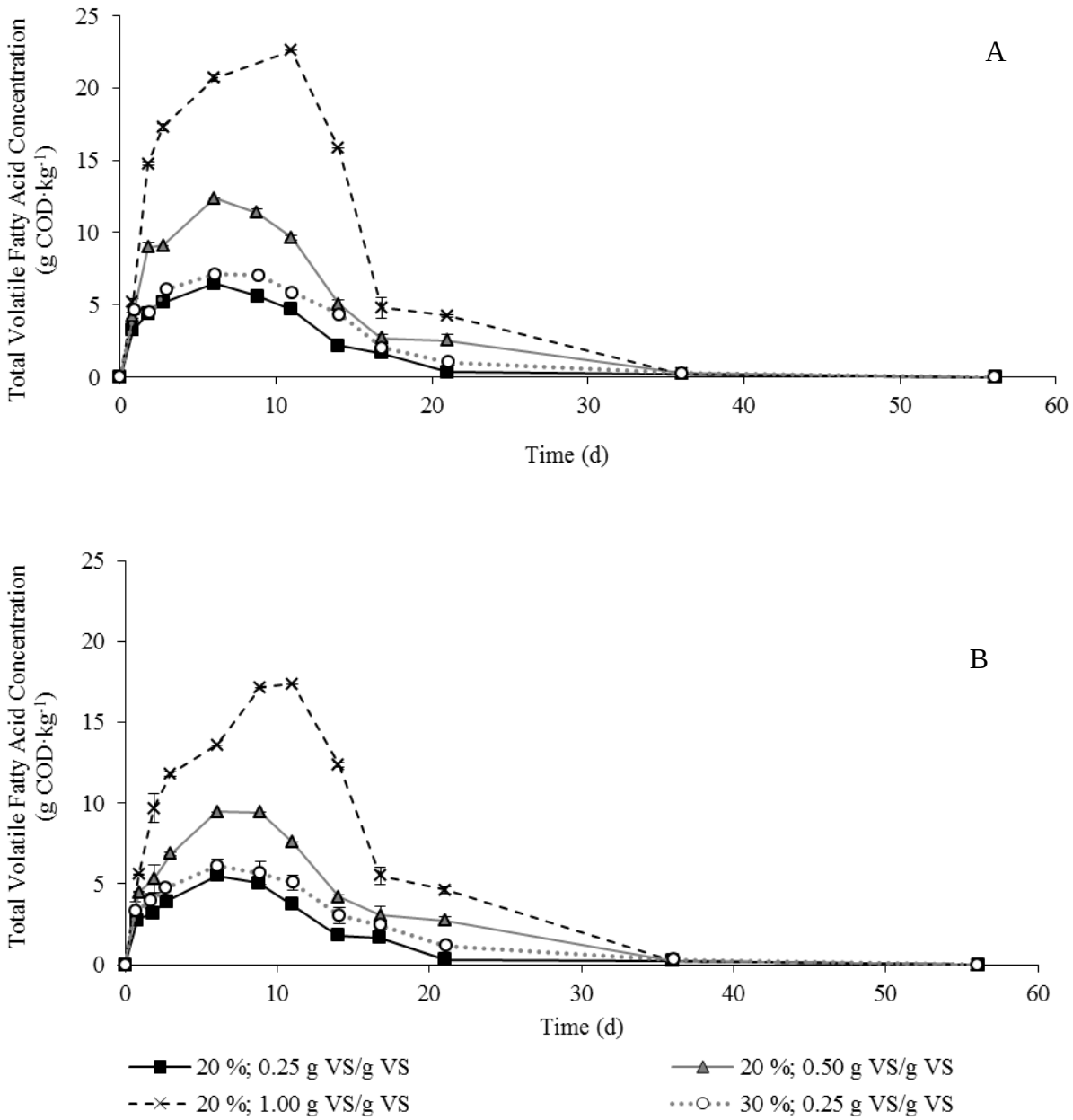

Figure 2. Concentration of total volatile fatty acids during anaerobic mono-digestion of food waste (A) and co-digestion of food waste and cardboard (B). The legend represents the operating conditions: total solid contents (%) and substrate to inoculum ratio (g VS·g VS^{-1})

Figure3

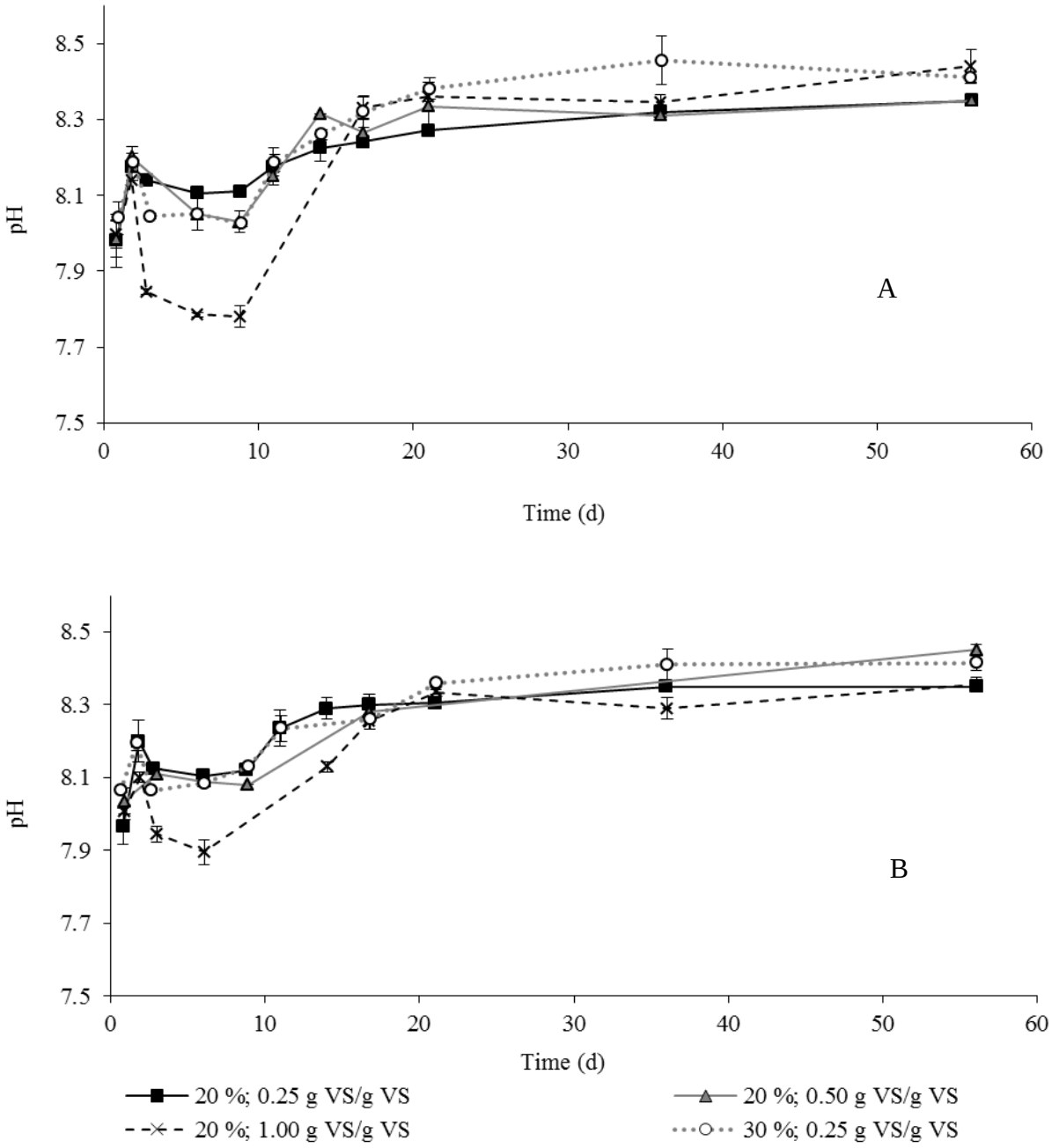

Figure 3. Evolution of the pH in the reactors during anaerobic mono-digestion of food waste (A) and co-digestion of food waste and cardboard (B). The legend represents the operating conditions: total solid contents (%) and substrate to inoculum ratio (g VS·g VS^{-1})

Figure4

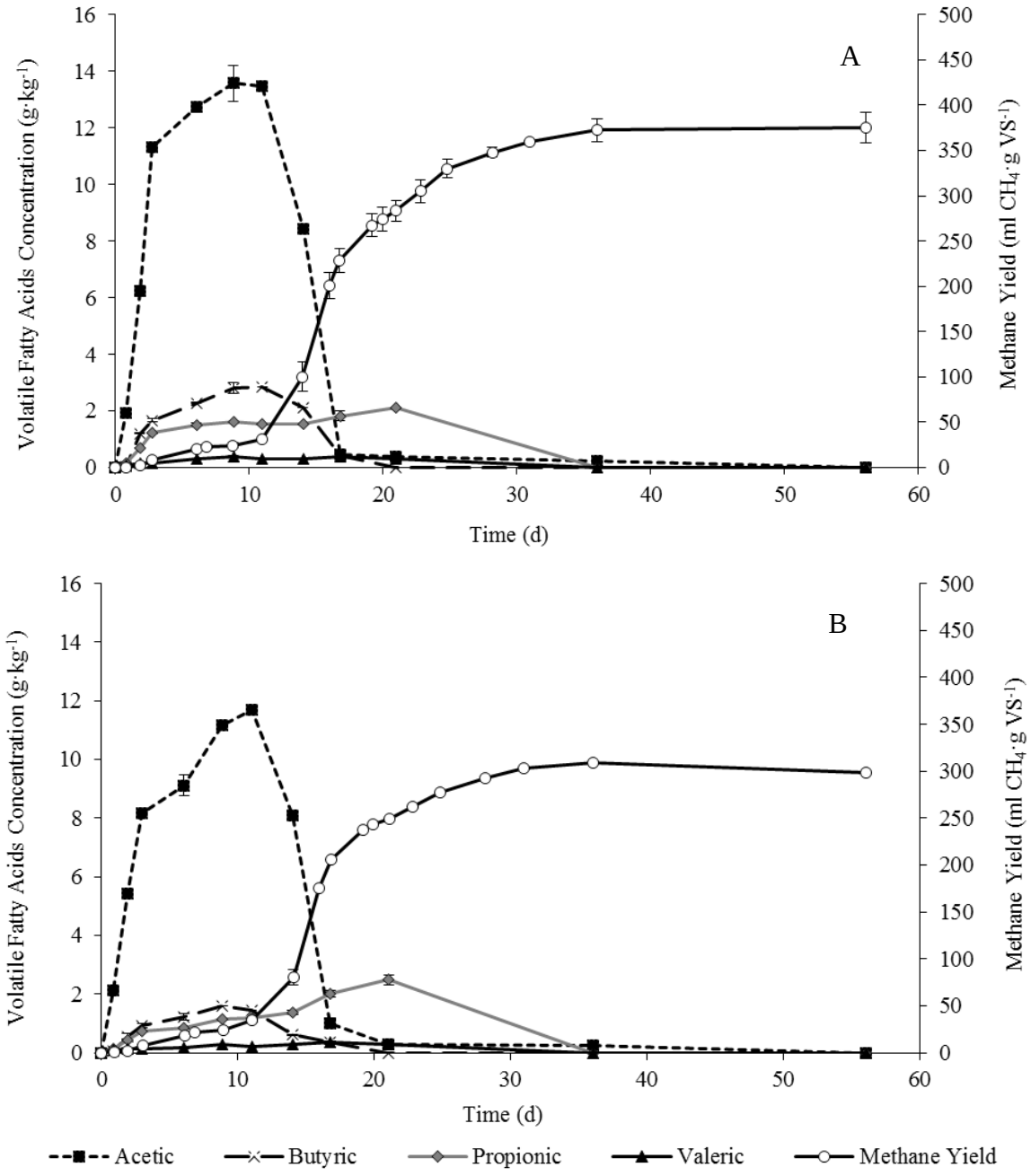

Figure 4. Concentrations of volatile fatty acids and methane yields during anaerobic digestion in reactor FW-20-1.00 (A; food waste mono-digestion; substrate to inoculum ratio of 1 g VS·g VS^{-1}; 20 % total solids) and reactor (FW+CB)-20-1.00 (B; food waste and cardboard co-digestion; substrate to inoculum ratio of 1 g VS·g VS^{-1}; 20 % total solids)